

RESEARCH LETTER

10.1002/2015GL064101

Key Points:

- Thermospheric Na layers above Syowa, for the first time at high latitudes
- Thermospheric Na layers extending up to 140 km with a wave-like structure
- Ionospheric/auroral conditions during the thermospheric Na layer event

Supporting Information:

• agutmpl_SI_Tsuda_20150402.pdf

Correspondence to:

T. T. Tsuda,
takuo.tsuda@uec.ac.jp

Citation:

Tsuda, T. T., X. Chu, T. Nakamura, M. K. Ejiri, T. D. Kawahara, A. S. Yukimatu, and K. Hosokawa (2015), A thermospheric Na layer event observed up to 140 km over Syowa Station (69.0°S, 39.6°E) in Antarctica, *Geophys. Res. Lett.*, *42*, 3647–3653, doi:10.1002/2015GL064101.

Received 2 APR 2015

Accepted 16 APR 2015

Accepted article online 22 APR 2015

Published online 18 May 2015

A thermospheric Na layer event observed up to 140 km over Syowa Station (69.0°S, 39.6°E) in Antarctica

T. T. Tsuda^{1,2,3}, X. Chu⁴, T. Nakamura^{1,5}, M. K. Ejiri^{1,5}, T. D. Kawahara⁶,
A. S. Yukimatu^{1,5}, and K. Hosokawa³

¹National Institute of Polar Research, Tachikawa, Japan, ²Research Fellow of Japan Society for the Promotion of Science, Japan, ³Department of Communication Engineering and Informatics, University of Electro-Communications, Chofu, Japan, ⁴Cooperative Institute for Research in Environmental Sciences and Department of Aerospace Engineering Sciences, University of Colorado at Boulder, Boulder, Colorado, USA, ⁵Department of Polar Science, Graduate University for Advanced Studies (SOKENDAI), Tachikawa, Japan, ⁶Faculty of Engineering, Shinshu University, Nagano, Japan

Abstract We report a thermospheric Na layer event (up to 140 km) observed by lidar in the night of 23–24 September 2000 at Syowa (69.0°S, 39.6°E), Antarctica. The thermospheric Na number densities were 2–9 cm⁻³ at 110–140 km, 3 orders of magnitude smaller than the peak density of the normal layer at 80–110 km. The thermospheric Na layers exhibited a wave-like structure with a period of 1–2 h. The colocated ionospheric/auroral observations showed sporadic *E* layers over Syowa through the night and an enhancement of the ionospheric/auroral activity around south side of Syowa at the event beginning. Adopting the theory by Chu et al. (2011), we hypothesize that the thermospheric Na layers are neutralized from converged Na⁺ layers. An envelope calculation shows good consistency with the observations.

1. Introduction

A number of observations of atmospheric metal layers, such as Na, Fe, and K layers, have been carried out by using resonance fluorescence lidars [cf. Chu and Papen, 2005, and references therein]. It is generally considered that these metal layers are normally distributed from 80 to 105 km. (Hereafter, the metal layer at 85–105 km is called the normal layer.) On the other hand, metal layers in the thermosphere (above 110 km) are one of the interesting subjects in the recent lidar studies [Gong et al., 2003; Höffner and Friedman, 2004, 2005; Chu et al., 2011; Wang et al., 2012; Friedman et al., 2013; Xue et al., 2013; Dou et al., 2013].

Höffner and Friedman [2004, 2005] studied an extension (up to 130 km) of the normal layer (at 80–105 km), what they called the mesospheric metal layer topside. More recently, Fe layers above 110 km up to 155 km were reported from Fe Boltzmann lidar observations at McMurdo Station (77.8°S, 166.7°E) in Antarctica [Chu et al., 2011]. The layers had distinct gravity wave signatures with periods of 1.5–2 h. The Fe layers (above 110 km) were called the thermospheric Fe layers. Although the Fe densities were low, ranging from 200 cm⁻³ at 120 km to 20 cm⁻³ at 150 km, compared with the normal layer peak density of 20,000 cm⁻³, they successfully obtained neutral temperature profiles from 110 to 150 km. The temperature at 115–135 km were considerably warmer than the modeled temperature and appeared to be related to Joule heating enhanced by auroral activity. Subsequently, a potassium (K) layer up to 155 km was reported from Arecibo Observatory (18.4°N, 66.8°W) [Friedman et al., 2013]. They showed that the layer, called the thermospheric K layer, descended with a speed of ~2.56 m s⁻¹ and that the descending speed was similar to the downward phase speed of the modeled semidiurnal tide over Arecibo.

There are several reports in Na layers up to 130 km from observations at Wuhan (31°N, 114°E) [Gong et al., 2003], Beijing (40.2°N, 116°E) [Wang et al., 2012], and Lijiang (26.7°N, 100.0°E) [Xue et al., 2013], China. These Na layers were called the double Na layers by Gong et al. [2003] and Wang et al. [2012], and the lower thermospheric-enhanced Na layers by Xue et al. [2013], respectively. Xue et al. [2013] showed a sporadic *E* (*E*_s) layer with large *f*_o*E*_s (up to 20 MHz) just before the lower thermospheric-enhanced Na layer event, and suggested relationship between the event and ion conversion due to tidal motions through the Na-ion chemistry. After that, Dou et al. [2013] reported statistical features of such kinds of layers based on observations at Beijing, Hefei (31.8°N, 117.3°E), Wuhan, and Haikou (19.5°N, 109.1°E). They showed that the layers were well correlated with *E*_s layers with *f*_o*E*_s larger than 4 MHz.

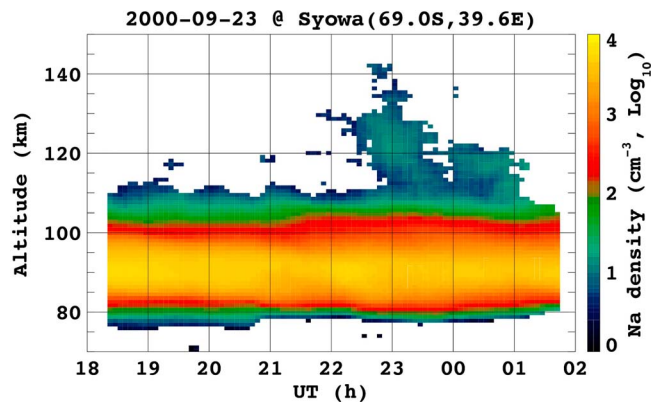


Figure 1. Time-altitude variations of Na number density from 18:00 UT on 23 September to 02:00 UT on 24 September 2000. The integration time and height are 30 min and 5 km, and the time and height intervals are 5 min and 1 km, respectively. Only data with errors (defined as one standard deviation) of less than 50% are displayed. It should be noted that the local time (LT) at Syowa Station is three hours ahead of UT, i.e., $LT = UT + 3 \text{ h}$ and that there is no difference between the magnetic local time (MLT) at Syowa Station and UT, i.e., $MLT = UT + 0 \text{ h}$.

2011] was regularly operated in 2000–2002 with the two-frequency technique [cf. *She et al.*, 1990] that was able to measure neutral temperature and Na density.

2. Observations

In this section, we present a thermospheric Na layer event observed on 23–24 September 2000, which was the only clear event found from the data sets of 246 nights during the three austral winter seasons (in 2000–2002). Then we report ionospheric/auroral conditions during the event, based on ionospheric/auroral observations with collocated instruments at Syowa Station.

Figure 1 shows time-altitude variation of the Na number density observed on 23–24 September 2000 at Syowa Station. The Na layer before 22:00 UT was distributed around 80–110 km, which was a typical normal Na layer in the height range. After that, thermospheric Na layers appeared above the normal Na layer. It is clearly found that significant signals were obtained up to 140 km in both laser frequencies during 22:00–24:00 UT (see Figure 2). The thermospheric Na layers consisted of two descending layers. The main body of the first

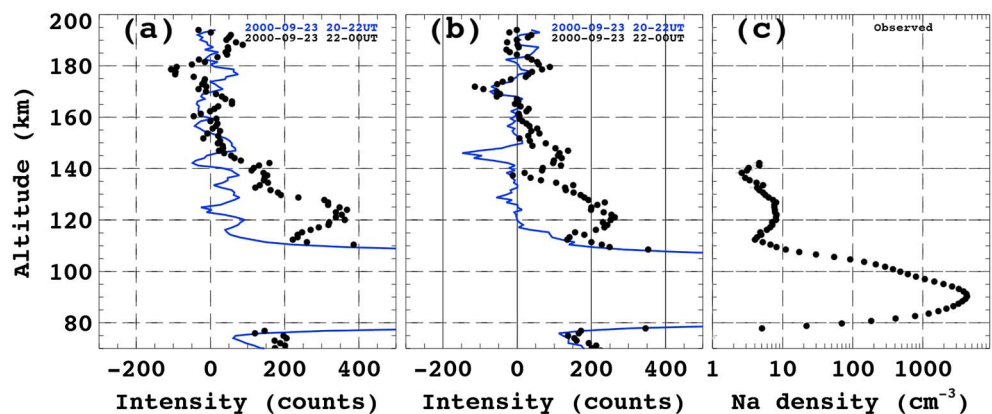


Figure 2. Comparison of signal intensities at periods during (black) and before (blue) the thermospheric Na layer event, which were obtained at two laser frequencies of (a) the Na D_{2a} peak and (b) the minimum between Na D_{2a} and D_{2b} peaks [cf. *Kawahara et al.*, 2011]. It should be noted that the background count, defined as averaged count from 160 to 200 km, are subtracted. Altitude profile of (c) Na density, calculated from 2 h integration data during the event (22:00–24:00 UT). Horizontal gray bars indicate a standard deviation error of each data. Concerning to the observational data in Figures 2a–2c), the integration time and height are 120 min and 5 km, respectively, and the height interval is 1 km.

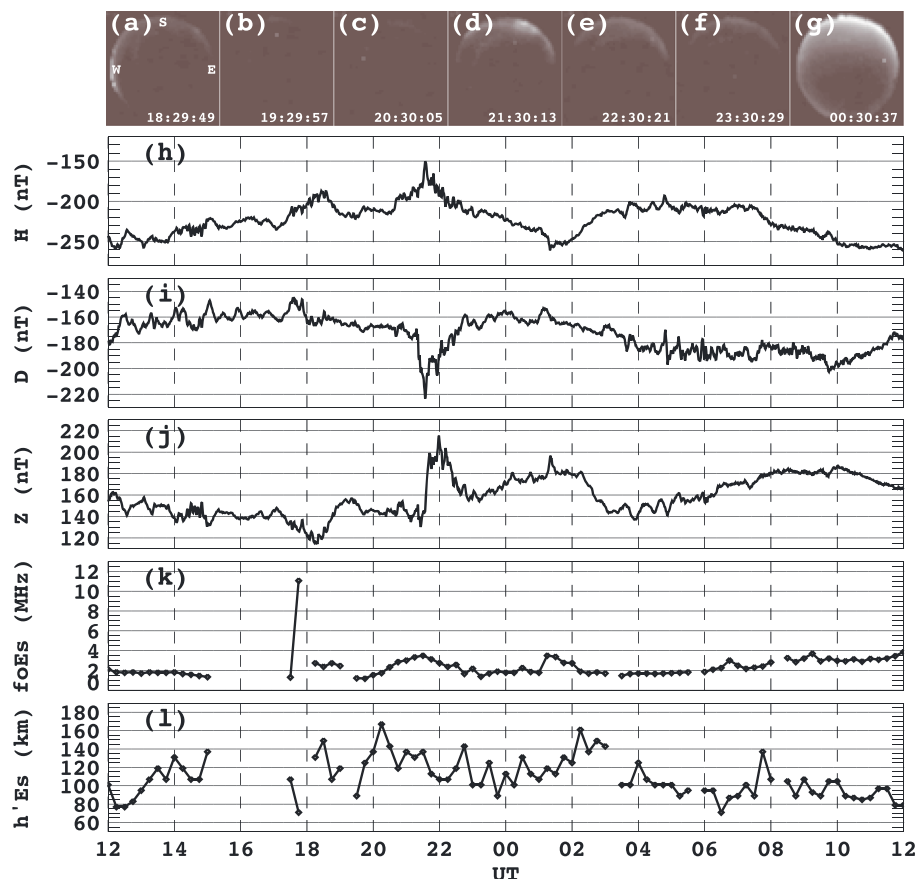


Figure 3. (a–g) All-sky images above Syowa Station, geomagnetic variations in (h) H, (i) D, and (j) Z components (corresponding to magnetic northward, eastward, downward components, respectively), and (k) f_oE_s and (l) $h'E_s$ determined from ionograms. It should be noted that the height information of the $h'E_s$ could be affected by a time delay, i.e., group retardation, in the radio propagation.

layer descended from 130 km to 110 km between 22:30 and 23:30 UT, and then merged with the normal layer. The descending speed was $\sim 5.6 \text{ m s}^{-1}$. The second layer appeared around 120 km at 24:00 UT, and then descended. These two descending layers showed a wave-like structure with a period of 1–2 h. The period was comparable to those of the gravity wave-like Fe layers observed at McMurdo Station [Chu *et al.*, 2011].

A vertical profile of Na number density during the event are shown in Figure 2. It should be noted that the data are derived from 2 h of integration data (between 22:00 and 24:00 UT) to increase the signal-to-noise ratio. The thermospheric layer (above the normal layer) was extending from 110 km up to 140 km. While the Na number density was quite low ($2\text{--}9 \text{ cm}^{-3}$), the density data were still significant compared with the error bars (defined as one standard deviation). The thermospheric Na density was 3 orders of magnitude smaller than that of the normal layer peak density (up to 4000 cm^{-3}). The ratio between the normal layer and thermospheric layer densities would resemble that in the case of the thermospheric Fe layer events [Chu *et al.*, 2011].

We have made a trial of neutral temperature data calculation above 110 km (not shown here), using the two-frequency technique (based on the Doppler measurement) [cf. She *et al.*, 1990]. The temperature errors (defined as one standard deviation) were huge (1000–10,000 K) above 110 km due to quite low Na density (less than 10 cm^{-3}), while the temperature data seemed to be fairly comparable to those from the NRLMSISE-00 model [Picone *et al.*, 2002]. Hence, the calculated temperature data would be unfortunately insignificant for the atmospheric science. However, this would be still meaningful as an important trial for future temperature measurements above 110 km, if we could largely improve the signal-to-noise ratio of

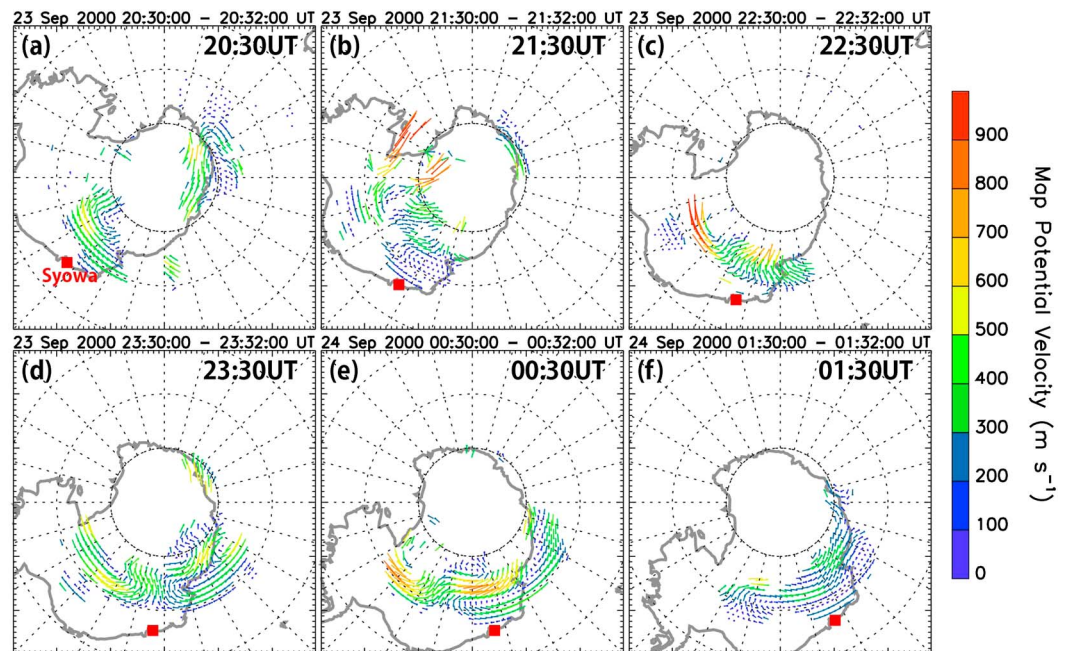


Figure 4. (a–f) SuperDARN ionospheric convection maps in the Southern polar region. The two-dimensional (2-D) ionospheric convection maps are created from the line-of-sight velocity data of the HF radars using the spherical harmonics fitting algorithm [cf. Ruohoniemi and Baker, 1998]. The location of Syowa Station is expressed as a red square.

the data in future lidar observations. Further interesting implication would be a possibility of wind velocity measurements above 110 km, because the Na Doppler lidar technique has a potential to measure the wind velocity [cf. Chu and Papen, 2005].

All-sky images on the same night indicated that there were no auroral emissions over Syowa Station during the night including the event period (see Figure 3), but there were weak auroral emissions at higher latitudes (south side of Syowa Station) around 21:30–22:30 UT. At almost the same time (around 21:00–23:00 UT), there were some geomagnetic variations, which would be related with the auroral activity at south side of Syowa Station. The relatively active period (21:00–23:00 UT) seemed to correspond to the beginning period of the thermospheric Na layer event (at 22:00–02:00 UT).

On the other hand, E_s layers occurred at all hours of nighttime on 23–24 September 2000. During the event period of 22:00–02:00 UT, the $h'E_s$ was 100–150 km and the f_oE_s was 2–4 MHz, respectively (see Figure 3). The $h'E_s$ was well consistent with the altitude of the observed thermospheric Na layer (i.e., 110–140 km). While the f_oE_s of 2–4 MHz was slightly smaller than (or similar to) that reported by the statistical study [Dou et al., 2013], the corresponding electron density was still high (approximately $5\text{--}20 \times 10^4 \text{ cm}^{-3}$). Thus, the electron density (i.e., ion density) above Syowa Station was quite high even without a presence of any auroral particle precipitations (indicated by the no auroral emissions). This implies that the positive ions would mainly consist of metal ions, such as Na^+ , with longer lifetimes compared with the normal major ions (i.e., NO^+ and O_2^+).

Figure 4 shows a sequence of ionospheric convection maps obtained from Super Dual Auroral Radar Network (SuperDARN) [Greenwald et al., 1995; Chisham et al., 2007] in the Southern Hemisphere. These maps have been derived by using a spherical harmonics fitting algorithm proposed by Ruohoniemi and Baker [1998]. In the vicinity of Syowa Station, the ionospheric convection was relatively weak before 21:30 UT. Then the convection was intensified with time from 22:30 UT. The period around 22:30 UT seemed to be corresponding to the beginning of the thermospheric Na layer event. During the period at 22:30–23:30 UT, Syowa Station was located close to the equatorward edge of the typical twin-cell convection pattern near midnight that corresponds to the exit of the antisunward plasma stream from the dayside toward the nightside across the central polar cap region.

3. Discussion

What causes the thermospheric metal layers is still an open question. *Chu et al.* [2011] suggested a hypothesis in the Fe, which is that neutral Fe layers are converted from converged Fe^+ layers. The hypothesis would be supported by reports in relationships between thermospheric Na layers and E_s layers (indicating the metal ion layers) [*Xue et al.*, 2013; *Dou et al.*, 2013]. On the other hand, an influence of the meteor shower activity on the thermospheric metal layers, suggested by *Höffner and Friedman*, 2004 [2004, 2005], has not been well proven and it cannot explain the high contrast of the observed neutral layers with the background. Here we briefly revisit the hypothesis by *Chu et al.* [2011] but for the case of Na with the information from the ionospheric/auroral observations, since we found E_s layers during our event as mentioned in the previous section.

The hypothesis examines the sources of the metal ion layers, the formation of the metal ion layers, and conversion from the ions to the neutrals. The first two issues concern the ion motions. Since the charge numbers are the same, the main difference between Na and Fe would be the mass. The Na mass (23 amu) is smaller than the Fe mass (56 amu), but the difference would not be so large (less than 1 order of magnitude). Thus, Na^+ is slightly more sensitive to the electromagnetic forcing (i.e., the Lorentz force). The important quantity in collision is the reduced mass, since these ions collide with N_2 (and O_2). The reduced masses for $\text{Na}^+\text{-N}_2$ and $\text{Fe}^+\text{-N}_2$ are 12.6 and 18.7 amu, which are pretty similar. Hence, the argument on Fe^+ can be applied to Na^+ . Vertical ion motion is basically controlled by the neutral wind and the electric field relative to the geomagnetic field lines [cf. *Kirkwood and von Zahn*, 1991]. In addition to this, the ionospheric current accompanied by the electric field may induce horizontal redistribution (including concentration) of the ions [*Matuura et al.*, 2013]. As mentioned in the previous section, we found the ionospheric/auroral activities at south side of Syowa Station around the onset of the event. The observed enhancement of the ionospheric convection indicates that the electric field became stronger. This can support the observed geomagnetic variations due to the ionospheric current. Furthermore, upward winds may be induced by Joule heating due to the ionospheric current. Thus, the intensified electric field can change the ion motions, and then may contribute to upward transportation and/or horizontal concentration of the ions. This may be the cause for the formation of the metal ion layers (including Na^+ layers) around above Syowa Station. The interpretation would be just a possibility or speculation, and more detailed analysis, e.g., using numerical simulations which includes combination of such multiple processes, is necessary for the correct evaluation, which is beyond the scope of the present paper.

The third issue (i.e., converting from the ions to the neutrals) concerns the metal chemistry. In the case of Fe [see *Chu et al.*, 2011], radiative recombination (i.e., $\text{Fe}^+ + e^- \rightarrow \text{Fe} + h\nu$) can produce neutral Fe above 120 km, and the reaction rate is $4\text{--}10 \times 10^{-12} \text{ cm}^3 \text{ s}^{-1}$. Assuming an E_s layer with a density of $1 \times 10^5 \text{ cm}^{-3}$, occupied with electrons and Fe^+ (without other ions), neutral Fe production rate is $4\text{--}10 \times 10^{-2} \text{ cm}^{-3} \text{ s}^{-1}$. Thus, the neutral Fe density of $40\text{--}100 \text{ cm}^{-3}$ can be produced with a time scale of 1000 s. The time scale was shorter than the wave period (5500 s), and the density was comparable to the observed density ($20\text{--}200 \text{ cm}^{-3}$). In the same manner but for the Na, the reaction rate of the radiative recombination (i.e., $\text{Na}^+ + e^- \rightarrow \text{Na} + h\nu$) is $1\text{--}4 \times 10^{-12} \text{ cm}^3 \text{ s}^{-1}$ when the electron temperature is 200–1000 K [*Pavlov*, 2012]. The electron density in the observed E_s layer was $5\text{--}20 \times 10^4 \text{ cm}^{-3}$. Assuming the Na^+ density of $5\text{--}20 \times 10^3 \text{ cm}^{-3}$ (1 order of magnitude smaller than the electron density [e.g., *Kopp*, 1997]), the production rate is $0.25\text{--}16 \times 10^{-3} \text{ cm}^{-3} \text{ s}^{-1}$, and then the Na density of $0.25\text{--}16 \text{ cm}^{-3}$ can be produced in a time scale of 1000 s, shorter than the observed wave period (1–2 h). The density was comparable to the observed Na density ($2\text{--}9 \text{ cm}^{-3}$). Therefore, these estimated results for the case of Na would not conflict with the hypothesis suggested by *Chu et al.* [2011].

As a final point, the present study comprises a few hours of observations on a single night, since we found only one clear event from all data in the Syowa Na lidar (i.e., the data sets of 246 nights during the three austral winter seasons in 2000–2002). On the other hand, such sporadic E layers (as seen in this event) are much more frequent, and thus, the thermospheric Na layers do not always appear in the presence of sporadic E layers. This point needs future investigation with more high-sensitive observations and numerical simulations.

4. Summary

The thermospheric metal layer is one of the interesting subjects in the recent resonance fluorescence lidar studies. There are several reports on this issue from low, middle, and high-latitude stations. In the present paper, we reported a thermospheric Na layer event above Syowa Station, for the first time observed at high

latitudes. The thermospheric Na layers exhibited a wave-like structure with a period of 1–2 h, which was similar to those of the thermospheric Fe layers reported previously from the high-latitude station, McMurdo [Chu *et al.*, 2011], but was different from those of the tidal waves suggested by the descending thermospheric layers observed at low-latitude stations, Arecibo Observatory and Lijiang [Friedman *et al.*, 2013; Xue *et al.*, 2013]. This may be due to the differences in dominant atmospheric wave activities among different sites.

From the colocated ionospheric/auroral observations, we have found that there were E_s layers over Syowa Station during the event and an enhancement of the ionospheric/auroral activity around south side of Syowa Station at the event beginning. Based on the observed ionospheric/auroral conditions as well as the theory by Chu *et al.* [2011], we hypothesize that the enhanced electric field contributes to the formation of the metal ion layers (including Na^+ layers) through the multiple processes (such as ion motion driver and heating source) and then the thermospheric Na layers are neutralized from converged Na^+ layers: $\text{Na}^+ + e^- \rightarrow \text{Na} + h\nu$.

As a future implication, of importance is that the thermospheric metal layers can provide valuable tracers to investigate atmospheric studies above 110 km. Actually, there is less information on neutral atmosphere at higher altitudes (above 110 km) due to lack of observational methods, except for some limited measurements (such as in situ measurements by rockets and limb-sounding by satellites). As mentioned above, Chu *et al.* [2011] have demonstrated the neutral temperature profiles from 110 to 150 km. The present study gives an implication for neutral temperature and wind velocity measurements by Na Doppler lidars. Thus, the thermospheric metal layers may open up a quite new understanding for the upper atmosphere above 110 km, such as atmospheric waves passing through the mesopause and auroral effects on the neutral atmosphere in the polar region.

Acknowledgments

The Na lidar observations from 2000 to 2002 were carried out as part of the Japanese Antarctic Research Expedition (JARE) observations. The auroral image data and the magnetometer data at Syowa Station were provided by the World Data Center (WDC) for Aurora in National Institute of Polar Research (NIPR). The ionosonde data were provided by WDC for Ionosphere, National Institute of Information and Communications Technology (NICT). The authors acknowledge the use of Super Dual Auroral Radar Network (SuperDARN) data. SuperDARN is a collection of radars funded by national scientific funding agencies of Australia, Canada, China, France, Japan, South Africa, United Kingdom, and United States of America. We thank A. Kadokura, NIPR, for supporting in the aurora image data and the magnetometer data and also thank T. Tsugawa, NICT, for supporting in the ionosonde data at Syowa Station. This research was supported by Japan Society for the Promotion of Science (JSPS) KAKENHI grants 25-526, 24340121, and 26610157, and partly supported by the joint research program of Solar-Terrestrial Environment Laboratory (STEL), Nagoya University. X. Chu was supported in part by the USA National Science Foundation grants ANT-0839091, PLR-1246405, and AGS-1136272.

The Editor thanks one anonymous reviewer for assisting in the evaluation of this paper.

References

- Chisham, G., *et al.* (2007), A decade of the Super Dual Auroral Radar Network (SuperDARN): Scientific achievements, new techniques and future directions, *Surv. Geophys.*, *28*(1), 33–109, doi:10.1007/s10712-007-9017-8.
- Chu, X., and G. C. Papen (2005), Resonance fluorescence lidar for measurements of the middle and upper atmosphere, in *The Book of Laser Remote Sensing*, edited by T. Fujii and T. Fukuchi, pp. 179–432, CRC Press, Taylor and Francis Group, Boca Raton, Fla.
- Chu, X., Z. Yu, C. S. Gardner, C. Chen, and W. Fong (2011), Lidar observations of neutral Fe layers and fast gravity waves in the thermosphere (110–155 km) at McMurdo (77.8°S, 166.7°E), Antarctica, *Geophys. Res. Lett.*, *38*, L23807, doi:10.1029/2011GL050016.
- Dou, X. K., S. C. Qiu, X. H. Xue, T. D. Chen, and B. Q. Ning (2013), Sporadic and thermospheric enhanced sodium layers observed by a lidar chain over China, *J. Geophys. Res. Space Physics*, *118*, 6627–6643, doi:10.1002/jgra.50579.
- Friedman, J. S., X. Chu, C. G. M. Burn, and X. Liu (2013), Observation of a thermospheric descending layer of neutral K over Arecibo, *J. Atmos. Sol. Terr. Phys.*, *104*, 253–259, doi:10.1016/j.jastp.2013.03.002.
- Gong, S., G. T. Yang, J. M. Wang, X. W. Cheng, F. Q. Li, and W. X. Wan (2003), A double sodium layer event observed over Wuhan, China by lidar, *Geophys. Res. Lett.*, *30*(5), 1209, doi:10.1029/2002GL016135.
- Greenwald, R. A., *et al.* (1995), DARN/SuperDARN: A global view of the dynamics of high-latitude convection, *Space Sci. Rev.*, *71*, 761–796, doi:10.1007/BF00751350.
- Höfner, J., and J. S. Friedman (2004), The mesospheric metal layer topside: A possible connection to meteoroids, *Atmos. Chem. Phys.*, *4*, 801–808, doi:10.5194/acp-4-801-2004.
- Höfner, J., and J. S. Friedman (2005), The mesospheric metal layer topside: Examples of simultaneous metal observations, *J. Atmos. Sol. Terr. Phys.*, *67*, 1226–1237, doi:10.1016/j.jastp.2005.06.010.
- Kawahara, T. D., T. Kitahara, F. Kobayashi, Y. Saito, A. Nomura, C.-Y. She, D. A. Krueger, and M. Tsutsumi (2002), Wintertime mesopause temperatures observed by lidar measurements over Syowa station (69°S, 39°E), Antarctica, *Geophys. Res. Lett.*, *29*(15), 4–1–4–4, doi:10.1029/2002GL015244.
- Kawahara, T. D., C. S. Gardner, and A. Nomura (2004), Observed temperature structure of the atmosphere above Syowa Station, Antarctica (69°S, 39°E), *J. Geophys. Res.*, *109*, D12103, doi:10.1029/2003JD003918.
- Kawahara, T. D., T. Kitahara, F. Kobayashi, Y. Saito, and A. Nomura (2011), Sodium temperature lidar based on injection seeded Nd:YAG pulse lasers using a sum-frequency generation technique, *Opt. Express*, *19*, 3553–3561.
- Kirkwood, S., and U. von Zahn (1991), On the role of auroral electric fields in the formation of low altitude sporadic-E and sudden sodium layers, *J. Atmos. Terr. Phys.*, *53*, 389–407, doi:10.1016/0021-9169(91)90034-5.
- Kopp, E. (1997), On the abundance of metal ions in the lower ionosphere, *J. Geophys. Res.*, *102*(A5), 9667–9674, doi:10.1029/97JA00384.
- Matuura, N., T. Tsuda, and S. Nozawa (2013), Field-aligned current loop model on formation of sporadic metal layers, *J. Geophys. Res. Space Physics*, *118*, 4628–4639, doi:10.1002/jgra.50414.
- Pavlov, A. V. (2012), Ion chemistry of the ionosphere at E- and F-region altitudes: Review, *Surv. Geophys.*, *33*, 1133–1172, doi:10.1007/s10712-012-9189-8.
- Picone, J. M., A. E. Hedin, D. P. Probst, and A. C. Aikin (2002), NRLMSISE-00 empirical model of the atmosphere: Statistical comparisons and scientific issues, *J. Geophys. Res.*, *107*(A12), 1468, doi:10.1029/2002JA009430.
- Ruohoniemi, J. M., and K. B. Baker (1998), Large-scale imaging of high-latitude convection with Super Dual Auroral Radar Network HF radar observations, *J. Geophys. Res.*, *103*(A9), 20,797–20,811, doi:10.1029/98JA01288.

- She, C. Y., H. Latifi, J. R. Yu, R. J. Alvares II, R. E. Bills, and C. S. Gardner (1990), Two-frequency lidar technique for mesospheric Na temperature measurements, *Geophys. Res. Lett.*, *17*, 929–932.
- Wang, J., Y. Yang, X. Cheng, G. Yang, S. Song, and S. Gong (2012), Double sodium layers observation over Beijing, China, *J. Geophys. Res.*, *39*, L15801, doi:10.1029/2012GL052134.
- Xue, X. H., X. K. Dou, J. Lei, J. S. Chen, Z. H. Ding, T. Li, Q. Gao, W. W. Tang, X. W. Cheng, and K. Wei (2013), Lower thermospheric enhanced sodium layers observed at low latitude and possible formation: Case studies, *J. Geophys. Res. Space Physics*, *118*, 2409–2418, doi:10.1002/jgra.50200.